

Systematic analysis of the direct methanol fuel cell

T. SCHULTZ¹, U. KREWER¹, T. VIDA KOVIĆ¹, M. PFAFFERODT², M. CHRISTOV^{1,3} and K. SUNDMACHER^{1,2,*}

¹Max Planck Institute for Dynamics of Complex Technical Systems, Sandtorstrasse 1, 39106, Magdeburg, Germany

²Otto-von-Guericke University Magdeburg, Process Systems Engineering Universitätsplatz 2, 39106, Magdeburg, Germany

³Department of Physical Chemistry, University of Chemical Technology and Metallurgy, 1756, Sofia, Bulgaria

(*author for correspondence, tel.: +49-391-6110-350, fax: +49-391-6119-353,

e-mail: sundmacher@mpi-magdeburg.mpg.de)

Key words: adsorption, crossover, direct methanol fuel cell, electrode kinetics, flowbed, model

Abstract

The dynamic operating behaviour of the direct methanol fuel cell (DMFC) is governed by several physico-chemical phenomena which occur simultaneously: double layer charging, electrode kinetics, mass transport inside the porous structures, reactant distributions in the anode and cathode flowbeds etc. Therefore it is essential to analyse the interactions of these phenomena in order to fully understand the DMFC. These phenomena were initially analysed independently by systematic experiments and model formulations. Electrode kinetics were determined by fitting models of varying complexity to electrochemical impedance spectroscopy (EIS) measurements. Reaction intermediates adsorbed on the catalyst seem to play a key role here. To describe mass transport across the DMFC a one-dimensional model was formulated applying the generalised Maxwell–Stefan equations for multi-component mass transport and a Flory–Huggins model for the activities of mobile species inside the membrane (PEM). Also swelling of the PEM as well as heat production and transport were considered. Finally, the anode flowbed was analysed by observing flow patterns in different flowbed designs and measuring residence time distributions (RTDs). Detailed CFD models as well as simpler CSTR network representations were used to compare to the experimental results. Even the simpler models showed good agreement with the experiments. After these investigations the results were combined: the electrode kinetics model was implemented in the mass transport model as well as in the CSTR network flowbed model. In both cases, good agreement, even to dynamic experiments, was obtained.

List of Symbols

c (mol m ⁻³)	Molar concentration
d (m)	Thickness
i (mA cm ⁻²)	Current density
n (mol m ⁻² s ⁻¹)	Overall molar flux density
r (mol m ⁻³ s ⁻¹)	Reaction rate
t (s)	Time
T (K)	Temperature
U (V)	Voltage
z (m)	Cell coordinate perpendicular to cell plane
Z (Ω)	Impedance

Greek symbols

α (–)	Charge transfer coefficient
η (V)	Overpotential
Θ (–)	Surface fraction
ϕ (V)	Electrical potential

Upper Indices

AC	Anode catalyst layer
AF	Anode feed
CC	Cathode catalyst layer
M	Membrane (PEM)

Lower Indices

a	Anode
c	Cathode
Cell	Cell
CH ₃ OH	Methanol
CO	Carbon monoxide
Dead	Due to experimental delays (“dead time”)
H ₂ O	Water
O	Oxygen

Abbreviations

CFD	Computational fluid dynamics
-----	------------------------------

CSTR	Continuously stirred tank reactor (i.e. lumped parameter model)
DMFC	Direct methanol fuel cell
EIS	Electrochemical impedance spectroscopy
PEM	Polymer electrolyte membrane

PEMFC	Polymer electrolyte membrane fuel cell
RTD	Residence time distribution
VCS	Electrode kinetics model according to [4]

1. Introduction

Since the early 1990s, the direct methanol fuel cell (DMFC) has gained significance as a portable supply of electrical power. Although the structure and materials are very similar to those of hydrogen-consuming polymer electrolyte fuel cells (PEMFC), the different nature of the anode reactants leads to a distinctly different operating behaviour and a variety of unique features, e.g. as discussed by Schultz et al. [1, 2] and Carrette et al. [3].

In order to identify and analyse the physico-chemical phenomena governing steady state and dynamic DMFC behaviour under real operating conditions, systematic experimental and simulation studies have been performed. The underlying strategy, the research areas, the chosen experimental and modelling approaches, and their main results will be presented here.

The research strategy was to first focus on individual phenomena; choosing appropriate experimental techniques to obtain data unaffected by other phenomena, formulating adequate models focusing on these phenomena and finally carrying out a systematic analysis with the aim of getting a clear understanding of these phenomena. The next step was then to combine those models to obtain more general models of the DMFC and to analyse the interaction of different phenomena. Appropriate dynamic experiments were designed and used for model validation as well as parameter identification.

The final aim of this research was to obtain realistic DMFC models of lowest possible complexity which describe the dynamic behaviour realistically.

2. Governing phenomena

Inside the DMFC, numerous coupled physico-chemical processes and phenomena occur simultaneously. These are

- methanol distribution in the anode flowbed structure,
- carbon dioxide removal from the anode flowbed,
- transport of methanol, water and carbon dioxide inside the anode diffusion layer (two-phase transport, as the solubility of carbon dioxide in water methanol solutions is not sufficient, which leads to carbon dioxide bubble formation),
- electrochemical methanol oxidation at the anode catalyst,

- transport of methanol, water and protons through the polymer electrolyte membrane (PEM),
- electrochemical oxygen reduction at the cathode catalyst,
- methanol oxidation at the cathode catalyst,
- transport of oxygen, water and carbon dioxide inside the cathode diffusion layer (possibly two-phase transport as water might condense),
- distribution of oxygen and removal of water inside the cathode flowbed structure and
- heat fluxes/heat management inside the DMFC structures.

Not all of these phenomena have the same impact on DMFC behaviour in different operating modes. For practical applications it is usually desired to operate the DMFC at medium current densities, where the power density is optimal and the likelihood of cathode flooding (i.e. water condensation in the cathode structures due to insufficient water removal) is minimised. For such low to medium current densities, condensation of water in the cathode structures can be neglected if a sufficient supply of dry air is ensured. Also the influence of carbon dioxide bubbles in the anode structures might be of minor influence, as long as the flow rate through the anode flowbed structure is sufficiently high and the current densities are in the low to medium range. Minimising the influence of both phenomena can be achieved by choosing appropriate experimental conditions.

Most of the phenomena of the above list have to be considered for all operating conditions, as illustrated in Figure 1. Therefore, the analysis of the DMFC is split up into separate tasks (decomposition of the problem).

The following tasks were addressed:

- analysis of the chemical and electrochemical reactions at both anode and cathode,

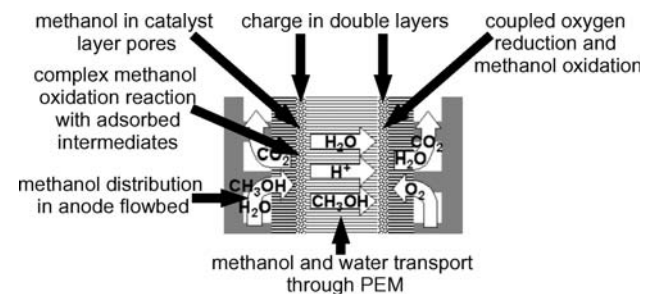


Fig. 1. Main phenomena governing DMFC behaviour.

- mass (and heat) transport inside the porous structures of the DMFC,
- flow distribution inside the anode flowbed.

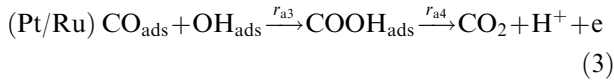
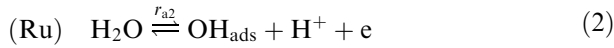
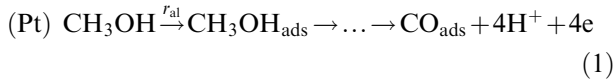
The approaches and main results of these topics will be presented, highlighting the progressive coupling of the individual results.

3. Electrode reaction mechanisms

Electrochemical anodic methanol oxidation, as well as cathodic oxygen reduction with coupled methanol oxidation, are complex reactions with multiple reaction intermediates bound to the metal catalysts. In order to obtain adequate, yet not too complex kinetic description for these reactions, different mechanisms of increasing complexity were postulated. Appropriate rate expressions were implemented in lumped models of the respective electrode or the complete DMFC.

3.1. Anodic methanol oxidation

For anodic methanol oxidation on platinum ruthenium catalysts the following reaction pathway is proposed [4, 5]:



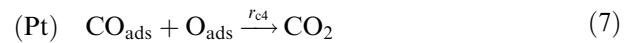
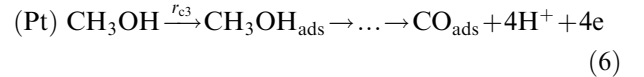
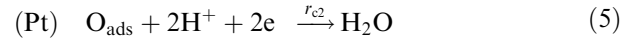
The reversible electrochemical adsorption of water on the ruthenium catalyst is described by a Butler–Volmer type rate expression. In the literature for the irreversible third reaction (Equation 3) two different mechanisms can be found: one proposed by Vidaković et al. [4] assumes a one step electrochemical interaction between OH_{ads} and CO_{ads} to be rate determining (referred to as VCS model), thus leading to a potential-dependent rate expression of Tafel type. The other mechanism proposed by Kauranen et al. [6] assumes the preceding surface reaction between CO_{ads} and OH_{ads} (r_{a3}) to be rate determining, leading to a potential-independent rate expression (referred to as the Kauranen model). As in all three reactions (Equations 1–3) adsorbed species occur, terms for adsorption/desorption also appear in all three kinetic expressions. These were assumed to be either of Langmuir or Temkin–Frumkin type (i.e. adsorption energies constant or functions of surface fractions, respectively).

With these two distinctions (VCS or Kauranen mechanism for third reaction, Langmuir or Temkin–Frumkin type adsorption kinetics), altogether four different model variants were obtained and implemented in a simple lumped model of the DMFC anode (mass balances for adsorbed CO and OH plus charge balance). For dynamic investigations, the model variants were linearised around the steady state and Laplace transformed to obtain transfer functions. Finally, these were transformed into the frequency domain, yielding the electrochemical impedance of the model variants.

To validate these model variants and to identify their parameters, steady state polarisation curves [4, 7] and electrochemical impedance spectra (EIS) [7] were recorded on real DMFC anodes using a cyclone flow cell [8, 9]. All four model variants produced equally good fits to the steady state experiments [4], and also qualitatively similar impedance spectra [5, 10]. But only the Kauranen model with Temkin–Frumkin adsorption rate expressions provided a quantitative fit to the experimental EIS (Figure 2) [5, 10].

3.2. Cathodic oxygen reduction with coupled methanol oxidation

A multi-step reaction mechanism with adsorbed intermediates was proposed for the anodic and cathodic reactions occurring simultaneously at the cathode [11]:



The reaction rates r_{c1} and r_{c4} were assumed to be potential-independent (i.e. adsorption and desorption steps, respectively) and described by Langmuir-type kinetic expressions. r_{c2} was assumed to be potential-dependent (Tafel type rate expression). Equation (6), finally, was assumed to represent a fast reaction, immediately consuming all methanol reaching the cathode. Therefore its reaction rate r_{c3} is identical to the methanol flux reaching the cathode.

The rate expressions and corresponding mass and charge balances were implemented in a DMFC model which is an extended version of the lumped DMFC anode model mentioned in the previous section. In this model, the PEM is a spatially

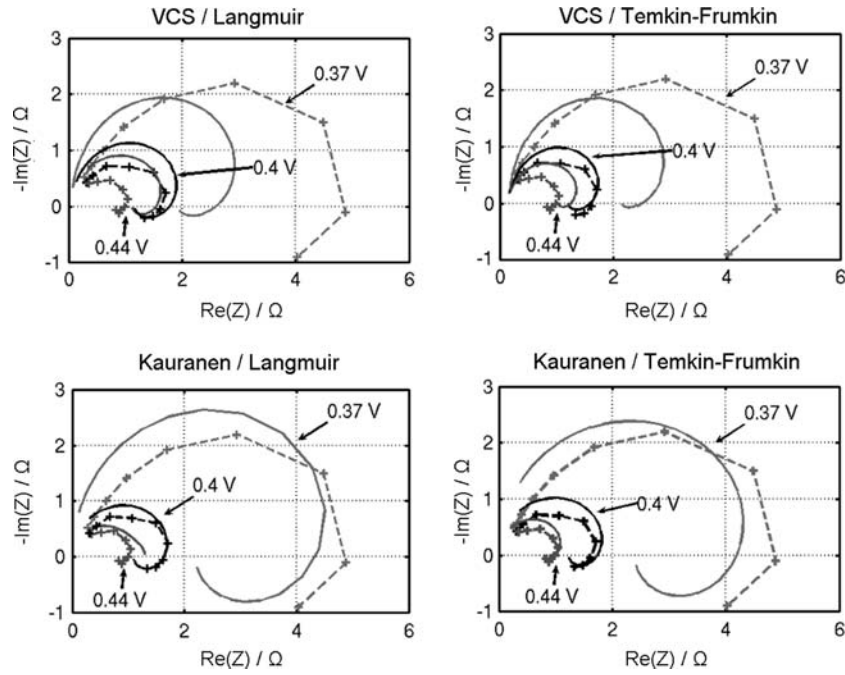


Fig. 2. Comparison of experimental (dashed lines) and simulated (solid lines) EIS for the four model variants.

distributed transport element for methanol (Fick diffusion approach with constant diffusivity used to describe mass transport). The parameters of this model were identified by fitting simulated cell voltage responses to methanol feed concentration step changes to experimental results [11]. The simulations were in fair agreement with the experimental results for increases in the methanol feed concentration, but could not describe the behaviour for decreasing feed concentrations. This subject will be further investigated in the future.

4. Transport processes inside the porous structures

Mass transport plays a significant role in the DMFC. Methanol crossover through the PEM reduces the efficiency, power density and long-term stability of the cathode catalyst, while methanol transport in the anode structures and oxygen transport in the cathode structures determine the limiting current densities and also possibly the cell performance for medium current densities.

In order to understand the governing transport processes, a detailed transport model was formulated and validated [1, 11, 12, 13]. It yields fair agreement with experimental steady-state crossover fluxes and cell voltages (Figure 3).

It can be concluded that this model, focusing on mass transport phenomena, is sufficient to describe most important features of a single cell DMFC in steady state. As will be shown later, for an adequate dynamic simulation more realistic rate expressions for the electrode reactions are necessary.

5. Flow distribution in anode flowbed

It is desirable to operate a DMFC at low anode feed flow rates in order to reduce the size of the anode feed pump. But the lower this flow rate, the more likely is maldistribution of methanol over the anode structure due to methanol consumption and carbon dioxide bubble formation. Maldistributions of methanol can also occur as a result of the flowbed design.

Such maldistributions can lead to areas with significantly different current densities and even the formation of inactive zones. As this is not desirable, the flowbed design, as well as the anode feed flow rate have to be analysed and optimised. Moreover, if a distinct methanol concentration distribution is inevitable, its effect on the overall cell behaviour has to be accounted for in realistic models.

5.1. Experiments

Experiments were carried out using acrylic cells into which different anode flow fields were machined. The inlet was fed with either pure water or water containing a coloured tracer. A desired flow rate was established with pure water and at a given time the feed was switched to the tracer solution. At the outlet the tracer concentration was monitored using a UV-VIS detector, while the whole flowbed was observed by a video camera [5, 14]. With the help of the UV-VIS detector the residence time distribution (RTD) was determined, while the video analysis allowed visualisation of the local concentration distribution by observing the movement of the tracer front and tracer concentration. Three different types of flowbeds typical for DMFCs were

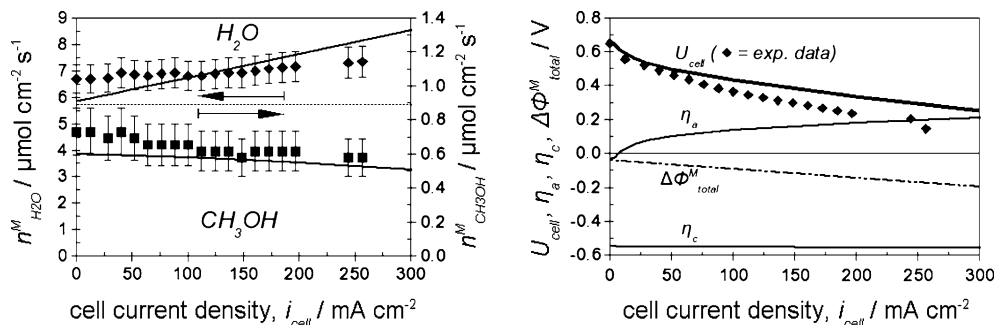


Fig. 3. Steady state experimental (symbols) and simulation results (mass transport model, solid lines). Left: Crossover flux densities of water and methanol through the PEM; right: Current voltage curve, anode and cathode overpotentials and potential drop over PEM. Operating conditions: cell temperature 75 °C; uniform cell pressure 1.7 bar; methanol feed concentration 1 mol dm⁻³; anode feed flow rate 0.5 dm⁻³ min⁻¹; cathode feed dry air with a dew point of 3 °C at a flow rate of 0.5 scbm h⁻¹.

analysed at various flow rates: two rectangular designs with parallel inlet and outlet distribution channels, connected by perpendicular parallel channels separated by solid walls (parallel channel design) or interrupted walls (spot design), and one rhomboidal design with triangular inlet and outlet distribution areas and parallel channels over the active area of the cell (rhomboidal design).

5.2. Model formulation and results

The model based analysis approached the problem from two sides. On one hand very simple models should represent the RTD experiments, while on the other hand the flowbed designs were implemented using a CFD software to get a high resolution representation of the flow behaviour comparable to that obtained from the video observations.

5.2.1. CFD simulations

The three flowbed geometries were implemented using the CFD software package CFX-5TM. The same conditions as in the experiments were used to carry out three-dimensional simulations. Figure 4 shows a typical result compared to the video experiment, proving a very good agreement between experiment and simulation. Obviously, CFD simulations are a powerful tool for flowbed optimisation. But on the other hand, the high complexity of a CFD model and the fixed structure of available model equations make it difficult to also include the porous structures of the DMFC. So for the simulation of the complete behaviour of a whole DMFC, simpler approaches are desirable.

5.2.2. CSTR network models

In order to get less complex flowbed models, the flowbeds were represented by networks of interconnected CSTRs [5] as shown in Figure 5.

Even with low numbers of CSTRs (Figure 5c) reasonable approximations to the flow distributions (Figure 5a) as well as to the experimental RTD (Figure 6) were obtained.

6. Coupling of individual models

The previous model approaches all focus on individual phenomena occurring inside the DMFC. Therefore none of them is able to explain the general behaviour of a DMFC, especially for complex realistic dynamic operating conditions like e.g. changes in methanol feed concentration. Therefore the detailed mass transport model discussed in section 4 was extended by stepwise introduction of the electrode kinetics derived in section 3, as extensively presented in Schultz and Sundmacher [11]. In order to compare these dynamic model variants, they were used to simulate a dynamic cell voltage response to a step change in the methanol feed concentration. The feed concentration was changed from an initial value of 1 or 1.5 mol dm⁻³ down to zero (i.e. to pure water feed) while all other operating conditions were kept constant, especially the cell current density. The cell voltage was recorded until the cell voltage broke down due to lack of fuel. Some sample results are presented in Figure 7 (left) [11]. It can be seen that the most simple model without reaction intermediates (Model I) predicts a much too fast cell voltage breakdown, while all other models with more realistic rate expressions at least manage to predict the sustaining time till the breakdown correctly. Model II with a more detailed anode rate expression accounting for adsorbed CO on the platinum catalyst can also predict cell voltage overshoots, if the cathode charge transfer coefficient is set to the relatively high value of $\alpha_c = 0.905$ (Model IIb). Model III with multi-step anode and cathode reaction mechanisms finally can predict overshoots with charge transfer coefficients of 0.5 on both anode and cathode side.

From the detailed analysis of those simulations [11], it can be concluded that the cell voltage overshoots result from the interaction of the anode and cathode overpotentials. The cathode overpotential is mainly influenced by the methanol crossover flux, decreasing significantly when the crossover flux ceases. Simultaneously, reaction intermediates adsorbed on the anode catalyst, reflux of methanol in the PEM, and unreacted

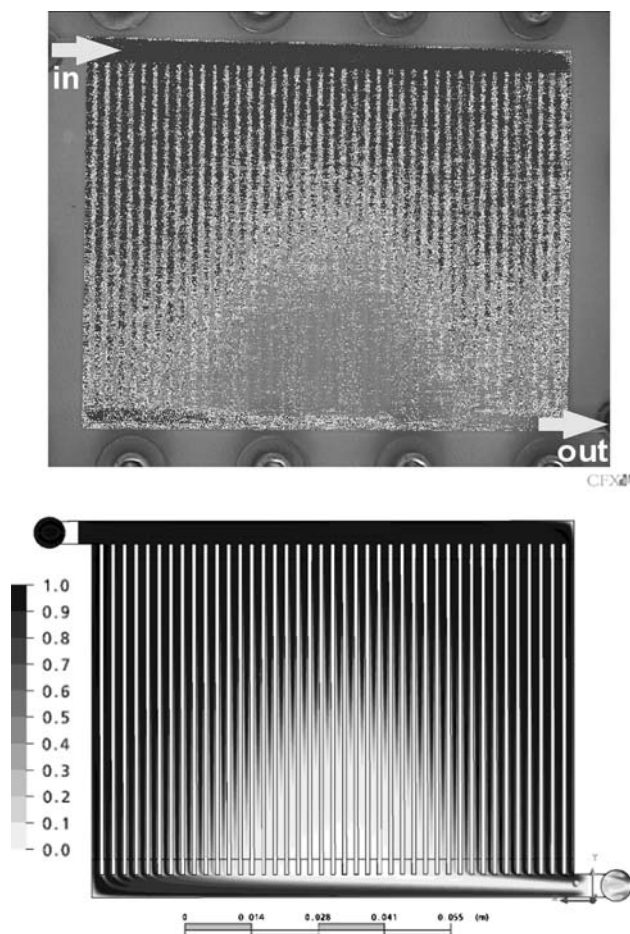


Fig. 4. Propagating tracer concentration fronts in parallel channel design flowbed: Experimental false color image (top) [5] and CFD simulation (bottom). In false color image the medium gray (lower centre) represents pure water.

methanol in the anode pore structure can supply the electrochemical anode reactions with reactants for a certain time, before the anode overpotential increases sharply due to educt shortage. The slow increase of the anode overpotential just after the feed switch, combined with the decrease in cathode overpotential due to ceasing methanol crossover, leads to the observed overshoots. In any case, the time for the overshoot to reach its maximum is not predicted correctly by Models I to III.

To overcome this, the complete anode reaction mechanism as presented in section 3 was implemented to obtain the model variant IV. In the simulations it was also checked how the real anode methanol feed concentration function influences the results. The feed switch valve is about 20 s upstream of the anode inlet at the chosen flow rate. Therefore it can be expected that at the anode inlet no sharp concentration step will be found, but a somewhat dispersed profile over time due to axial dispersion. In a first, simple, test a linear decrease over 20 s was used as inlet concentration function instead of the immediate drop. The result is presented in Figure 8. A much better fit to the experimental data was achieved, even for higher current densities where no overshoot occurs. Therefore, Model IV (i.e. the combination of the

complete mass transport model (section 4) with the detailed reaction kinetics model (section 3) is a powerful model for describing the dynamic behaviour of the DMFC.

6.1. Coupling of CSTR network models with electrode kinetics

In order to analyse possible interactions of electrode kinetics and methanol distribution in the anode flowbed, the electrode kinetics (=lumped DMFC) model from section 3 was combined with the CSTR network model presented in section 6 [5, 15]. To each CSTR representing one element of the active area of the anode flowbed, one set of equations of the electrode kinetics model was attributed. The cell voltage was assumed to be the same in each element, leading to individual local current densities. The total current is the sum of all local currents.

With this model family, the same current density step changes were simulated as with the lumped DMFC model (section 3) and for all simulations one single set of model parameters was identified. Some sample results are presented in Figure 9. Here experimental cell voltage

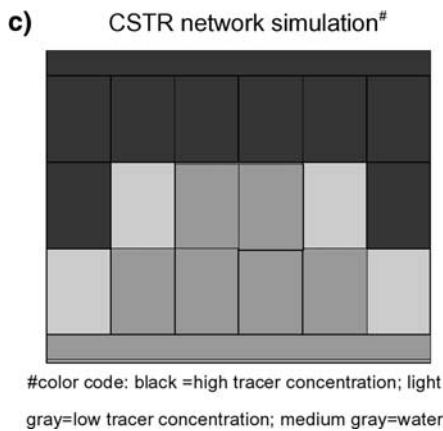
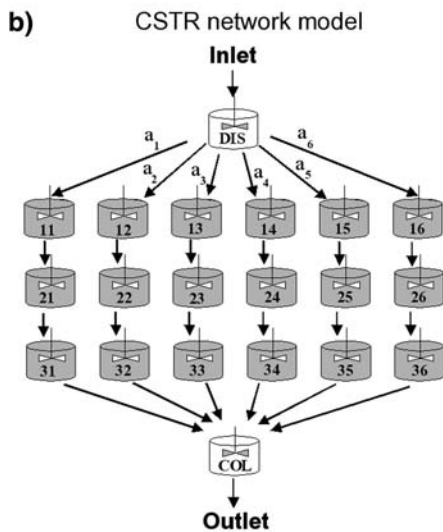
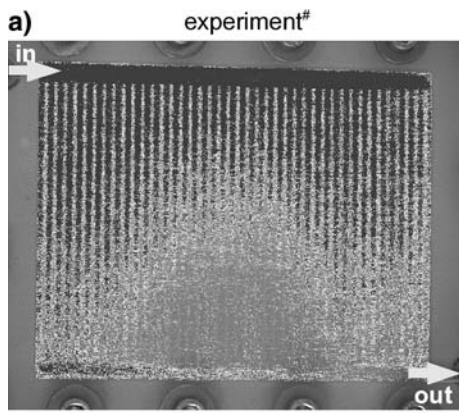


Fig. 5. Parallel channel design flowbed represented by CSTR network.

responses (Figure 9, left) to a step-down in the cell current at different anode feed flow rates are compared to simulation results (Figure 9, right) obtained from the combined model. The figure shows the results for the parallel channel design, but quite similar results were found for the other two flowbed designs.

The model has the same time constants as the experiment. After 1–2 s the maximum of the cell voltage overshoot is reached; after 5–6 more seconds a new steady state is established. Another agreement between

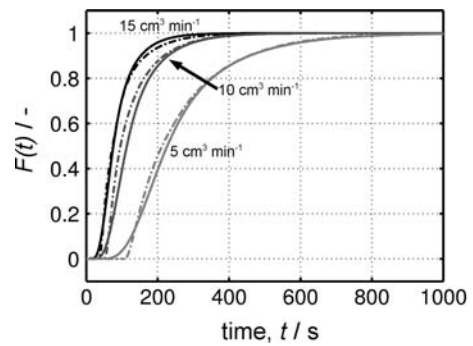


Fig. 6. Experimental (dash dotted lines) and simulated (solid lines) cumulative residence time distributions (RTD) of the parallel channel design for different volumetric flow rates.

experiments and simulation is that for lower anode feed flow rates the overshoot height decreases. For the lowest flow rates measured ($1 \text{ cm}^3 \text{ min}^{-1}$) the model predicts no overshoot at all. The reason for this behaviour is the decreasing methanol concentration in the anode catalyst layer for decreasing feed flow rates at the same current densities. This leads to changes in surface coverage which result in increased anode overpotentials.

The experiments and simulations mainly differ in the steady state cell voltages and the differences between flowbed designs. For low flow rates the simulation predicts a slight decrease in steady state cell voltage with increasing anode flow rate. For higher flow rates ($50 \text{ cm}^3 \text{ min}^{-1}$ and above) a constant limiting value is obtained. In contrast, the experiments show an almost linear increase in steady state cell voltage even for such high flow rates.

With respect to flowbed design, within the chosen operating conditions, only a small influence on the simulated current voltage curves and dynamic cell voltage responses was found in the simulations [5, 15], while in the experiments differences between the flowbed designs were found at least for medium to high current densities.

Those two major differences between experiments and simulations can be attributed to the fact that carbon dioxide bubble formation (whose impact on the DMFC behaviour increases with current density) is neglected in the models.

7. Conclusions

The present analysis has led to an enhanced understanding of many important physico-chemical phenomena responsible for the complex dynamic operating behaviour of a DMFC. Powerful models were developed and linked, providing a reasonable fit to many steady state and dynamic experimental observations. Systematic analysis also yielded hints for possible model reduction for certain operating regimes. This is a sound basis for the design and analysis of process control systems for real DMFCs. Also, based on these models,

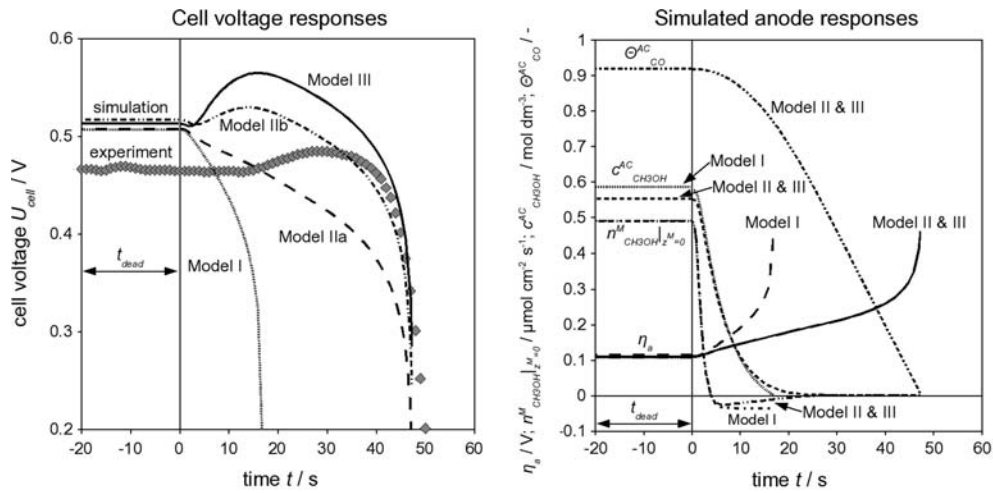


Fig. 7. Left: Comparison of simulated (lines) and experimental (symbols) cell voltage responses to a change in anode feed concentration from 1 mol dm^{-3} down to zero (i.e. pure water) for constant cell current density of $i_{cell} = 56 \text{ mA cm}^{-2}$; right: Corresponding anode responses of different model variants (operating conditions as given in [11]).

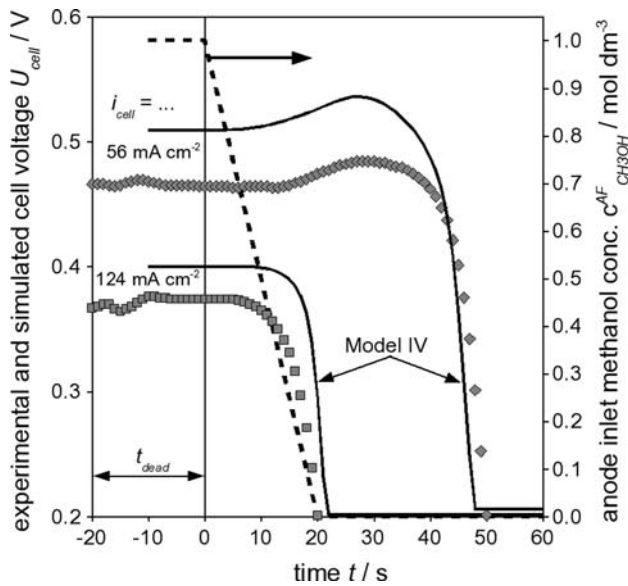


Fig. 8. Comparison of simulated (solid lines) and experimental (symbols) cell voltages for Model IV, using the inlet concentration profile given by the dashed line (instead of an immediate step down to zero) (operating conditions as given in [11] cell current density $i_{cell} = 56 \text{ mA cm}^{-2}$).

so-called state observers can be designed for non-measurable quantities like e.g. crossover fluxes, electrode potentials, membrane hydration state etc., as is already under way for high temperature fuel cells [16]. These can play an important role in online process analysis.

Nonetheless, not all phenomena possibly influencing DMFC behaviour are accounted for, like e.g. carbon dioxide bubble formation on the anode side and possible condensation of water on the cathode side. Also not all aspects of the models are experimentally validated, like heat production and transport and cathode reaction kinetics. Even the postulated anode reaction mechanism is not precisely validated, although its model implementation yields good fits for EIS and even enables the more complex models to achieve realistic system responses to dynamic operating conditions. Further experiments and simulations will aim at analysing the DMFC anode response to perturbations in the electrode potential much larger than those applied in EIS measurements. Such non-linear impedance spectroscopy will also have to analyse the higher harmonics of the system cell current response.

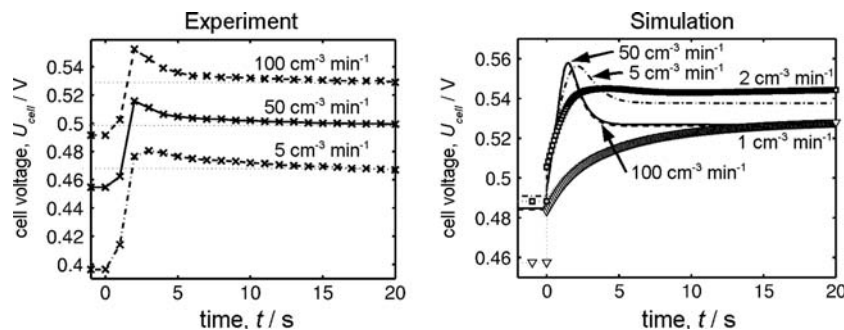


Fig. 9. Experimental (left) and simulated (right) cell voltage responses to a step change in the cell current density from 52 mA cm^{-2} down to 26 mA cm^{-2} (anode flow rates: $1 \text{ cm}^{-3} \text{ min}^{-1}$ triangles; $2 \text{ cm}^{-3} \text{ min}^{-1}$ squares; $5 \text{ cm}^{-3} \text{ min}^{-1}$ dash dotted; $50 \text{ cm}^{-3} \text{ min}^{-1}$ solid; $100 \text{ cm}^{-3} \text{ min}^{-1}$ dashed).

References

1. T. Schultz, Experimental and Model based Analysis of the Steady state and Dynamic Operating Behaviour of the Direct Methanol Fuel Cell (DMFC), Dissertation (Otto von Guericke University, Magdeburg, 2004). Free download: <http://www.diglib.uni-magdeburg.de/Dissertationen/2004/thoschultz.htm>.
2. T. Schultz, S. Zhou and K. Sundmacher, *Chem. Eng. Technol.* **24** (2001) 1223.
3. L. Carrette, K.A. Friedrich and U. Stimming, *Fuel Cells* **1** (2001) 5.
4. T. Vidaković, M. Christov and K. Sundmacher, *J. Electroanal. Chem.* **580** (2005) 105.
5. U. Krewer, System oriented analysis of the dynamic behaviour of direct methanol fuel cells, Dissertation (Otto von Guericke University, Magdeburg, 2005). Free download: <http://www.diglib.uni-magdeburg.de/Dissertationen/2005/ulrkrewer.htm>.
6. P.S. Kauranen, E. Skou and J. Munk, *J. Electroanal. Chem.* **404** (1996) 1.
7. T. Vidaković, Kinetics of methanol electrooxidation on PtRu catalysts in a membrane electrode assembly, Dissertation (Otto von Guericke University, Magdeburg, 2005). Free download: <http://www.diglib.uni-magdeburg.de/Dissertationen/2004/tanvidaković.htm>.
8. K. Sundmacher, *J. Appl. Electrochem.* **29** (1999) 919.
9. T. Vidaković, M. Christov and K. Sundmacher, *Electrochim. Acta* **49** (2004) 2179.
10. U. Krewer, M. Christov, T. Vidaković and K. Sundmacher, *J. Electroanal. Chem.* **589** (2006) 148.
11. T. Schultz and K. Sundmacher, *J. Power Sources* accepted, 2006.
12. T. Schultz and K. Sundmacher, *J. Power Sources* **145** (2005) 435.
13. T. Schultz and K. Sundmacher, *J. Memb. Sci.* **276** (2006) 272.
14. U. Krewer, Y. Song, V. John, R. Luebke, G. Matthies, K. Sundmacher and L. Tobiska, *Chem. Eng. Sci.* **59** (2004) 119.
15. U. Krewer, A. Kamat and K. Sundmacher, *J. Electrochem. Soc.* submitted.
16. M. Mangold, M. Grotzsch and A. Kienle, *J. Process Control*, submitted.